

# Insights into the Electronic Structure of Disulfur Tetrafluoride Isomers from Generalized Valence Bond Theory

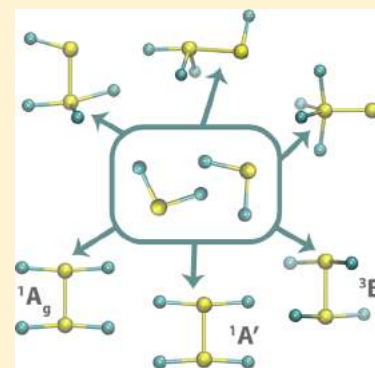
Beth A. Lindquist,<sup>†</sup> Alaina L. Engdahl,<sup>‡</sup> David E. Woon,<sup>†</sup> and Thom H. Dunning, Jr.\*<sup>‡,§,†</sup>

<sup>†</sup>Department of Chemistry, University of Illinois at Urbana–Champaign, 601 S. Mathews Avenue, Urbana, Illinois 61801, United States

<sup>‡</sup>Department of Chemistry, Wittenberg University, Springfield, Ohio 45504, United States

## Supporting Information

**ABSTRACT:** Sulfur and fluorine can participate in a variety of bonding motifs, lending significant diversity to their chemistry. Prior work has identified three distinct minima for disulfur tetrafluoride ( $S_2F_4$ ) compounds: two  $FSSF_3$  isomers and one  $SSF_4$  species. We used a combination of sophisticated explicitly correlated coupled cluster calculations and generalized valence bond (GVB) theory to characterize the electronic structure of these species as well as additional stationary points on the potential energy surface with  $F_2SSF_2$  connectivity. On the singlet surface, the two stationary points considered in this work with an  $F_2SSF_2$  structure are first- or second-order saddle points and not minima. However, on the triplet surface, we discovered a novel  $C_2$  symmetric  $F_2SSF_2$  minimum that was anticipated from the structure of an excited state ( ${}^3B_1$ ) of  $SF_2$ . Analysis using the GVB wave function in conjunction with the recoupled pair bonding model developed by our group provides a straightforward explanation of the bonding in all of the  $S_2F_4$  structures considered here. In addition, the model predicted the existence of the  $F_2SSF_2({}^3B)$  minimum.



## I. INTRODUCTION

Sulfur and fluorine combine to create a multitude of compounds. While  $SF_6$  is by far the most ubiquitous  $S_nF_m$  compound, there are many other species with varying degrees of stability that demonstrate the remarkable richness of sulfur–fluorine chemistry. While  $SF_6$  is stable enough to use as an insulator in transformers, the related  $S_2F_{10}$  is so toxic it has been considered as a potential chemical warfare agent.<sup>1</sup> A study by Steudel et al.<sup>2</sup> enumerated stable sulfur fluorides for all positive formal oxidation states of sulfur (+0–6), in addition to the theoretically characterizing three distinct minima for disulfur tetrafluoride ( $S_2F_4$ ). As reported in their study, these  $S_2F_4$  isomers possess significant structural variability, including a range of disulfide bond lengths: 1.9, 2.1, and 2.2 Å.<sup>2</sup> This diversity has interesting implications for the reactivity of sulfur fluorides. For instance, the lowest-energy  $S_2F_4$  species, here denoted  $FSSF_3$  (a), is the experimentally observed product of  $SF_2$  dimerization;<sup>3</sup> however, such experiments are complicated by the tendency of  $FSSF_3$  to react further to form other sulfur fluorides.<sup>4</sup> One counterintuitive property of  $FSSF_3$  (a) is that the longest S–F bond does not break in the lowest-energy pathway to dissociation into two  $SF_2$  molecules.<sup>2</sup> In a previous publication, we explained this finding by locating a very shallow, higher-lying local minima that complicates the potential energy surface as this S–F bond is broken in  $FSSF_3$  (a).<sup>5</sup> On the whole, diversity and complexity seem to be hallmarks of sulfur fluoride chemistry.

This variability in terms of connectivity and structure is a consequence of the array of bonding schemes in which sulfur

and fluorine can participate. In addition to typical polar covalent bonds, our group has shown that the properties of these two atoms are well-suited to forming recoupled pair bonds.<sup>6</sup> A recoupled pair bond is formed via an interaction between the singlet-coupled electrons in a lone pair on an atom with an electron in a singly occupied orbital on an incoming ligand. For sulfur fluorides, the  $2p^1$  orbital of a F atom can interact with the  $3p^2$  lone pair of sulfur and sometimes (depending on whether it is accessible to the ligand) the  $3s^2$  pair as well.<sup>7</sup> We have shown that ligand electronegativity is directly correlated with the strength of recoupled pair bonds formed with the S  $3p^2$  pair, so fluorine is ideal in this regard.<sup>8</sup> The energetic favorability of recoupled pair bond dyads, in which both electrons from an atomic lone pair form bonds with two ligands, leads to interesting features in many sulfur fluorides. For the example of  $FSSF_3$  (a) discussed above, we found that the connection between S–F bond length and reactivity was muddled by recoupled pair bonding. In the same study, we found that the S–F bond lengths and strengths in  $FSSF_3$  (a) are not inversely correlated with one another, and we found that recoupled pair bonding explained this surprising property as well.<sup>5</sup>

The variety of bonding motifs available to sulfur fluorides is manifest in even the  $SF_2$  molecule, in which there are two low-lying excited states in addition to the ground state. Our group

**Received:** August 23, 2014

**Revised:** September 30, 2014

**Published:** October 1, 2014



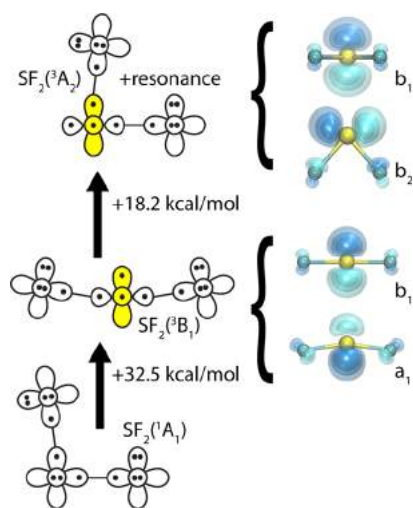


**Figure 1.** GVB diagrams for the  ${}^1A_1$  ground state, the  ${}^3B_1$  and  ${}^3A_2$  excited states of  $SF_2$ , as well as the singly occupied orbitals of the triplet states. Yellow shading indicates that the orbitals are triplet coupled. Throughout, the sulfur atom is yellow and the fluorine atom is cyan.

has previously described the bonding in these states;<sup>7</sup> their relative energetics and corresponding orbital diagrams are shown in Figure 1. Briefly, the ground  ${}^1A_1$  state is the straightforward result of the formation of two polar covalent S–F bonds involving the two *singly occupied* orbitals of the  $S(3P)$  atom. The first excited state of  $SF_2$  is of  ${}^3B_1$  symmetry and is the result of two F atoms interacting with the *doubly occupied* orbital of  $S(3P)$  as shown in Figure 1. This bonding motif is an example of a recoupled pair bond dyad: the two electrons of the  $S 3p^2$  pair are recoupled to form two S–F bonds. The triplet-coupled orbitals are modified from the singly occupied orbitals present in the  $S(3P)$  atom, as the slightly bent F–S–F angle slightly distorts the  $a_1$  symmetric orbital. (These orbitals are shown in Figure 1 as well.) The second excited state has  ${}^3A_2$  symmetry and is a resonance mixture of two types of bonds: one covalent S–F bond involving a singly occupied orbital of sulfur and one recoupled pair S–F bond with the  $S 3p^2$  pair. Of the triplet-coupled pair, the  $b_1$  symmetric orbital is again essentially an  $S 3p$  orbital, and the  $b_2$  symmetric orbital is the remaining orbital from the  $S 3p^2$  pair symmetrically distributed by resonance interactions. Our prior studies have found that recoupled pair bond dyads are particularly stable, owing to the reduction of Pauli repulsion between the electrons residing in sulfur-centered orbitals; the  ${}^3B_1$  state lies only 32.5 kcal/mol above the ground state. This is why the  ${}^3B_1$  state is lower in energy than the  ${}^3A_2$  state. In this work, we will show that the presence of these low-lying excited states of  $SF_2$  influences the geometries and energetics of larger sulfur fluorides such as  $S_2F_4$ .

In this work, we used generalized valence bond (GVB) calculations to understand the nature of the bonding in previously reported structures of  $S_2F_4$ , and we describe a novel minimum on the triplet surface with  $F_2SSF_2$  connectivity that has no counterpart on the singlet surface. Lower levels of theory find closed-shell  $F_2SSF_2$  structures that are bound,<sup>3</sup> but these structures were shown to be saddle points at higher levels of theory.<sup>2</sup> However, these stationary points do have S–S bond lengths characteristic of single bonds; therefore, we will analyze these species as well. In Section II, we review our computational methodology. In Section III, we consider the three

isomers of  $S_2F_4$  previously found by Steudel et al.,<sup>2</sup> as well as the behavior of the  $F_2SSF_2$  structures on the singlet and triplet surfaces. Finally, we conclude in Section IV.

## II. COMPUTATIONAL METHODOLOGY

Most calculations in this work were carried out with the Molpro suite of quantum chemical programs,<sup>9</sup> with the exception of the density functional theory (DFT) calculations, which were performed in Gaussian.<sup>10</sup> For the DFT calculations, the Becke hybrid functional<sup>11</sup> and the exchange-correlation functional of Lee, Yang, and Parr,<sup>12</sup> together denoted B3LYP,<sup>13</sup> were used. B3LYP calculations using the augmented correlation-consistent basis set of triple- $\zeta$  quality (aug-cc-pVTZ)<sup>14,15</sup> were used to optimize geometries and calculate frequencies. For the energetics, the Molpro CCSD(T)-F12 program or its spin-restricted counterpart, RCCSD(T)-F12, with the “a” approximation was used.<sup>16–19</sup> By explicitly including terms that depend on interelectronic distances in the wave function, convergence with respect to basis set size is accelerated.<sup>20</sup> Unless otherwise noted, all calculations with Molpro were performed with the aug-cc-pVTZ basis set with an extra set of tight d-functions on the sulfur atom [aug-cc-pV(T+d)Z].<sup>21</sup>

To elucidate the nature of the bonding in the  $S_2F_4$  isomers, generalized valence bond (GVB) calculations were performed using the CASVB program of Cooper and co-workers as implemented in Molpro.<sup>22,23</sup> (The full GVB wave function is identical to the SCVB wave function of Gerratt et al.<sup>24</sup>) The GVB wave function is particularly useful because the orbitals are singly occupied, atomic-like, and unique; therefore, the changes in the orbitals resulting from bond formation can be easily interpreted to provide unprecedented insights into the nature of the bonding. The GVB wave function is a product of spatial functions (the orbitals) that is multiplied by a sum of spin functions appropriate for the given number of electrons ( $N$ ) and spin state ( $S$ ). Orbitals are partitioned into two types: (1) active orbitals, which are singly occupied, allowed to overlap with each other, and all associated spin couplings are included, and (2) inactive orbitals, which are treated equivalently to molecular orbitals. That is, they are coupled into singlet pairs with only the spin function  $\alpha\beta$  included in the wave function; the paired orbitals have unit overlap but are orthogonal to all other orbitals. For  $2N_d$  inactive orbitals and  $N_a$  active orbitals, the GVB wave function is

$$\Psi_{\text{GVB}} = \hat{A}(\phi_{d1}\phi_{d1}\cdots\phi_{dN_d}\phi_{dN_d}\varphi_{a1}\varphi_{a2}\cdots\varphi_{aN_a}\alpha\beta\cdots\alpha\beta\Theta_{S,M}^{N_a})$$

where  $\{\phi_{di}\}$  are the inactive orbitals and  $\{\varphi_{ai}\}$  are the active orbitals;  $\Theta_{S,M}^{N_a} = \sum_k c_{sk} \Theta_{S,M,k}^{N_a}$  is the sum of all spin functions associated with the active electrons. In this work, we used the Kotani spin basis.  $\hat{A}$  is the antisymmetrizer, which ensures that the wave function satisfies the Pauli principle.

In this work, one term in  $\Theta_{S,M}^{N_a}$ , that which pairs the electrons successively into singlets, or the perfect pairing spin function, dominates ( $w_{\text{pp}} > 90\%$ ) the wave function at the equilibrium geometries of the molecules. (See Table S1 of the Supporting Information.) This simplifies our interpretation of the GVB orbital overlaps: (1) overlaps between orbitals in which the electrons are singlet coupled are energetically favorable, representing Heitler–London bond pairs<sup>25</sup> when the two orbitals are centered on different atoms, and (2) overlaps between orbitals in which the electrons are not singlet-coupled are repulsive because of the Pauli exclusion principle.<sup>26–29</sup> In

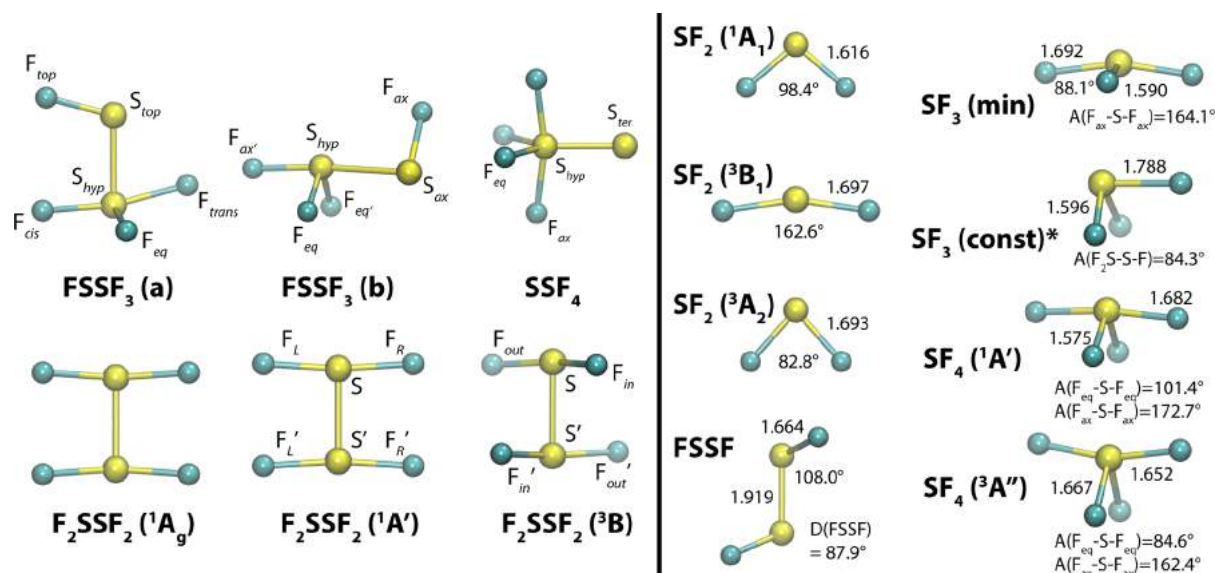


**Figure 2.** Structures for all molecules discussed in the text, atom labels for the S<sub>2</sub>F<sub>4</sub> species, and geometric parameters for the smaller sulfur fluorides. Bond lengths are given in angstroms. F<sub>2</sub>SSF<sub>2</sub> (<sup>1</sup>A') is a transition state, and F<sub>2</sub>SSF<sub>2</sub> (<sup>1</sup>A<sub>g</sub>) is a second-order saddle point. In SF<sub>3</sub> (const), the bond angle formed by the short (1.596 Å) S–F bonds is fixed at its value in SF<sub>2</sub> (<sup>1</sup>A<sub>1</sub>).

**Table 1. Geometrical Parameters [B3LYP/aug-cc-pVTZ] for (a) the Two FSSF<sub>3</sub> Isomers and SSF<sub>4</sub> and (b) the F<sub>2</sub>SSF<sub>2</sub> Geometries Examined in This Work**

(a)			
	FSSF <sub>3</sub> (a)	FSSF <sub>3</sub> (b)	SSF <sub>4</sub>
R(SS)	2.080	2.242	1.904
R(FS)	1.620 (F <sub>top</sub> –S <sub>top</sub> )	1.649 (F <sub>ax</sub> –S <sub>ax</sub> )	1.641 (F <sub>ax</sub> –S <sub>hyp</sub> )
	1.673 (F <sub>cis</sub> –S <sub>hyp</sub> )	1.706 (F' <sub>ax</sub> –S <sub>hyp</sub> )	1.589 (F <sub>eq</sub> –S <sub>hyp</sub> )
	1.600 (F <sub>eq</sub> –S <sub>hyp</sub> )	1.594 (F <sub>eq</sub> –S <sub>hyp</sub> )	
	1.767 (F <sub>trans</sub> –S <sub>hyp</sub> )	1.590 (F' <sub>eq</sub> –S <sub>hyp</sub> )	
A(FSS)	105.3 (F <sub>top</sub> –S <sub>top</sub> –S <sub>hyp</sub> )	90.4 (F <sub>ax</sub> –S <sub>ax</sub> –S <sub>hyp</sub> )	97.0 (F <sub>ax</sub> –S <sub>hyp</sub> –S <sub>ter</sub> )
	93.4 (F <sub>cis</sub> –S <sub>hyp</sub> –S <sub>top</sub> )	173.2 (F' <sub>ax</sub> –S <sub>hyp</sub> –S <sub>ax</sub> )	127.6 (F <sub>eq</sub> –S <sub>hyp</sub> –S <sub>ter</sub> )
	107.2 (F <sub>eq</sub> –S <sub>hyp</sub> –S <sub>top</sub> )	87.0 (F <sub>eq</sub> –S <sub>hyp</sub> –S <sub>ax</sub> )	
A(FSF)	75.3 (F <sub>trans</sub> –S <sub>hyp</sub> –S <sub>top</sub> )	93.6 (F' <sub>eq</sub> –S <sub>hyp</sub> –S <sub>ax</sub> )	
	166.7 (F <sub>cis</sub> –S <sub>hyp</sub> –F <sub>trans</sub> )	100.2 (F' <sub>eq</sub> –S <sub>hyp</sub> –F <sub>eq</sub> )	103.7 (F <sub>eq</sub> –S <sub>hyp</sub> –F <sub>eq</sub> )
	89.2 (F <sub>cis</sub> –S <sub>hyp</sub> –F <sub>eq</sub> )	86.2 (F <sub>ax</sub> –S <sub>hyp</sub> –F <sub>eq</sub> )	165.8 (F <sub>ax</sub> –S <sub>hyp</sub> –F <sub>ax</sub> )
	87.6 (F <sub>trans</sub> –S <sub>hyp</sub> –F <sub>eq</sub> )	87.8 (F' <sub>ax</sub> –S <sub>hyp</sub> –F <sub>eq</sub> )	85.6 (F <sub>ax</sub> –S <sub>hyp</sub> –F <sub>eq</sub> )
τ(FSSF)	–4.4 (F <sub>cis</sub> –S <sub>hyp</sub> –S <sub>top</sub> –F <sub>top</sub> )	–158.1 (F' <sub>ax</sub> –S <sub>hyp</sub> –S <sub>ax</sub> –F <sub>ax</sub> )	
	–94.6 (F <sub>eq</sub> –S <sub>hyp</sub> –S <sub>top</sub> –F <sub>top</sub> )	–159.2 (F' <sub>ax</sub> –S <sub>hyp</sub> –S <sub>ax</sub> –F <sub>ax</sub> )	
	–177.3 (F <sub>trans</sub> –S <sub>hyp</sub> –S <sub>top</sub> –F <sub>top</sub> )	100.7 (F' <sub>ax</sub> –S <sub>hyp</sub> –S <sub>ax</sub> –F <sub>ax</sub> )	
(b)			
	F <sub>2</sub> SSF <sub>2</sub> ( <sup>1</sup> A <sub>g</sub> )	F <sub>2</sub> SSF <sub>2</sub> ( <sup>1</sup> A')	F <sub>2</sub> SSF <sub>2</sub> ( <sup>3</sup> B)
R(SS)	2.102	2.100	2.171
R(FS)	1.703	1.702	1.711 (F <sub>in</sub> –S)
			1.719 (F <sub>out</sub> –S)
A(FSS)	93.7	94.0	88.2 (F <sub>in</sub> –S–S')
			87.1 (F <sub>out</sub> –S–S')
A(FSF)	172.7	159.4	161.4
τ(FSSF)		161.0 (F' <sub>L</sub> –S'–S–F <sub>R</sub> )	80.0 (F <sub>in</sub> –S–S'–F' <sub>in</sub> )
			–81.9 (F <sub>out</sub> –S–S'–F' <sub>in</sub> )
			116.1 (F <sub>out</sub> –S–S'–F' <sub>in</sub> )

this work, the orbitals that are plotted in the figures constitute the active space for the calculation.

The GVB calculations were started from (and the inactive orbitals taken as) Hartree–Fock (HF) orbitals localized with the Pipek–Mezey<sup>30</sup> criterion. More details on GVB theory can be found in several detailed reviews on the subject.<sup>24,31,32</sup> Additionally, all reported charges for the S<sub>2</sub>F<sub>4</sub> isomers are

calculated from a Mulliken analysis of the GVB wave function, with the charges of the smaller sulfur fluorides calculated from a Mulliken analysis of the HF wave function. For all charges reported in the main text for the S<sub>2</sub>F<sub>4</sub> isomers, comparison to the analogous natural bond order (NBO)<sup>33</sup> charges is made in Table S2 of the Supporting Information, where we find the same qualitative trends for both types of population analyses.

### III. RESULTS

The structures, atom labels, and selected geometric parameters of the various sulfur fluorides of interest in this work are shown in Figure 2, with the remaining geometric parameters reported in Table 1. On the left of Figure 2 are the  $S_2F_4$  isomers, and on the right are smaller sulfur fluorides that can be viewed as their precursors. The two FSSF<sub>3</sub> structures and SSF<sub>4</sub> are in qualitative agreement with those obtained from the MP2-(full)/6-31G\* calculations in the previous study of Steudel et al.,<sup>2</sup> though there are some minor differences in the geometric parameters. The majority of the bond lengths agree to within 0.04 Å, and bond angles generally agree to within 2.0°, though some of the more flexible dihedral angles deviate more significantly. For the geometry optimizations, we used density functional calculations (B3LYP) to balance accuracy and computational cost; we calculated the energetics of the resulting structures with accurate CCSD(T)-F12 calculations. Compared to very accurate coupled cluster calculations [RCCSD(T)/aug-cc-pV(Q+d)Z] reported in prior work<sup>7</sup> for SF<sub>3</sub>(min) and SF<sub>3</sub>(<sup>1</sup>A'), the bond lengths reported here are a little longer (0.02–0.04 Å) with similar bond and dihedral angles (within 1°). As indicated in Table S3 of the Supporting Information, we found deviations in that same range between the DFT-optimized structure of FSSF<sub>3</sub>(a) and the structure optimized with a coupled cluster calculation. Despite these small geometric differences, the two FSSF<sub>3</sub>(a) structures differed in energy by only 1.9 kcal/mol [CCSD(T)-F12/aug-cc-pV(T+d)Z]. Therefore, the minor differences in our structures are expected to have only a small impact on the energetics, and they will certainly not change our qualitative description of the bonding in these species. The relative energetics of the various  $S_2F_4$  species are given in Table 2,

**Table 2. Relative Energetics of the Various  $S_2F_4$  Species Discussed in the Text, Where the Zero of Energy Is Two SF<sub>2</sub>(<sup>1</sup>A<sub>1</sub>) Molecules**

$S_2F_4$ species	relative energy (kcal/mol)
FSSF <sub>3</sub> (a)	−20.3
SSF <sub>4</sub>	−13.4
FSSF <sub>3</sub> (b)	−2.3
F <sub>2</sub> SSF <sub>2</sub> ( <sup>1</sup> A') <sup>a</sup>	+27.8
F <sub>2</sub> SSF <sub>2</sub> ( <sup>1</sup> A <sub>g</sub> ) <sup>b</sup>	+29.5
F <sub>2</sub> SSF <sub>2</sub> ( <sup>3</sup> B)	+36.0
2 × SF <sub>2</sub> ( <sup>3</sup> B <sub>1</sub> )	+65.0

<sup>a</sup>Transition state. <sup>b</sup>Second-order saddle point.

where the zero of energy is two SF<sub>2</sub>(<sup>1</sup>A<sub>1</sub>) molecules. In agreement with ref 2, we find that FSSF<sub>3</sub>(a) is the global minimum, followed by SSF<sub>4</sub>, then FSSF<sub>3</sub>(b). The additional structures with F<sub>2</sub>SSF<sub>2</sub> connectivity lie significantly higher in energy. On the singlet surface, the F<sub>2</sub>SSF<sub>2</sub> structures are saddle points; however, there is a true minimum on the triplet surface for the F<sub>2</sub>SSF<sub>2</sub>(<sup>3</sup>B) state.

One prominent feature apparent from Table 1a,b is the range of values for the S–S bonds in the  $S_2F_4$  isomers. From the sum of the covalent radii for two sulfur atoms,<sup>34</sup> the expected length for a single S–S σ bond is 2.10 ± 0.04 Å. While many of the species have S–S bond lengths within or close to this range, there are some noteworthy deviations. SSF<sub>4</sub>, for example, has a very short S–S bond length (1.904 Å). This is in line with other S–S bonds that are often drawn as double bonds based on their shortness, such as the ground (<sup>3</sup>Σ<sub>g</sub><sup>−</sup>) state of S<sub>2</sub> (1.913 Å). In

**Table 3. Bond Lengths and Dissociation Energies for Disulfide Bonds, Calculated with Respect to the Given Asymptote**

	R <sub>c</sub> (SS) (Å)	D <sub>c</sub> (SS) (kcal/mol)
FS( <sup>2</sup> Π) + SF <sub>3</sub> (min) → FSSF <sub>3</sub> (a)	2.080	56.1
FS( <sup>2</sup> Π) + SF <sub>3</sub> (const) <sup>a</sup> → FSSF <sub>3</sub> (b)	2.242	53.3
S( <sup>1</sup> D) + SF <sub>4</sub> ( <sup>1</sup> A')	1.904	63.2
S( <sup>3</sup> P) + SF <sub>4</sub> ( <sup>3</sup> A'')	1.904	129.4
SF <sub>2</sub> ( <sup>3</sup> B <sub>1</sub> ) + SF <sub>2</sub> ( <sup>3</sup> B <sub>1</sub> ) → F <sub>2</sub> SSF <sub>2</sub> ( <sup>1</sup> A') <sup>b</sup>	2.100	37.3
SF <sub>2</sub> ( <sup>3</sup> B <sub>1</sub> ) + SF <sub>2</sub> ( <sup>3</sup> B <sub>1</sub> ) → F <sub>2</sub> SSF <sub>2</sub> ( <sup>1</sup> A <sub>g</sub> ) <sup>c</sup>	2.102	35.5
SF <sub>2</sub> ( <sup>3</sup> B <sub>1</sub> ) + SF <sub>2</sub> ( <sup>3</sup> B <sub>1</sub> ) → F <sub>2</sub> SSF <sub>2</sub> ( <sup>3</sup> B)	2.171	29.1

<sup>a</sup>F–S–F angle constrained to its value in SF<sub>2</sub>(<sup>1</sup>A<sub>1</sub>). <sup>b</sup>Transition state. <sup>c</sup>Second-order saddle point.

Section C, we will address the reasons for the shortness of this bond. On the other hand, FSSF<sub>3</sub>(b) contains a long S–S bond (2.242 Å), which we will discuss in Section B. Table 3 collects all of the S–S bond lengths as well as the corresponding bond dissociation energies with respect to the relevant asymptote(s). These latter values also have significant variance, suggesting diverse bonding motifs for the S–S bonds. In the following subsections, we will describe the bonding associated with the geometries shown in Figure 2, using GVB theory and the recoupled pair bonding model to understand the variations in the molecular properties.

**A. FSSF<sub>3</sub>(a).** The most stable  $S_2F_4$  isomer is FSSF<sub>3</sub>(a), which possesses C<sub>1</sub> symmetry and exhibits pronounced asymmetry in the S<sub>hyp</sub>–F<sub>trans</sub> and S<sub>hyp</sub>–F<sub>cis</sub> bonds.<sup>35</sup> Furthermore, significant barriers are present (see below) for rotation of the F<sub>top</sub>–S<sub>top</sub>–S<sub>hyp</sub>–F<sub>eq</sub> dihedral angle. This is consistent with the experimental observation that interconversion of F<sub>cis</sub> and F<sub>trans</sub> does not occur appreciably at room temperature.<sup>36</sup> We can explain these features by way of our previous analysis of the GVB wave function for this isomer, in which we showed that the axial bonds of FSSF<sub>3</sub>(a) form a F<sub>cis</sub>–S<sub>hyp</sub>–F<sub>trans</sub> recoupled pair bond dyad. That is, two F atoms are bonded to the electrons in the 3p<sup>2</sup>-like lone pair of one of the S atoms in FSSF.<sup>5</sup> Equivalently, the electronic structure can be viewed as a F atom (F<sub>eq</sub>) and an SF fragment (S<sub>top</sub>–F<sub>top</sub>) bonding covalently to the singly occupied orbitals of SF<sub>2</sub>(<sup>3</sup>B<sub>1</sub>); see Figure 1 for reference.

Because of the connection between FSSF and FSSF<sub>3</sub>, they have some similar properties. In FSSF, there is also a significant barrier to rotation of the dihedral angle (~30 kcal/mol), attributable to the polarization of the S 3p<sup>2</sup>-like pairs toward the opposite sulfur atom; the electron-deficient region on the sulfur side of the S–F bond allows these lone pairs to delocalize over both S atoms. Because of the extensive delocalization of those orbitals, convergence of the GVB wave function to a physically reasonable solution is difficult. Therefore, the Hartree–Fock orbitals for these electron pairs are shown in Figure 3a, where it is apparent that these molecular orbitals (MOs) possess a significant amount of π bonding character, resulting in a short (1.919 Å) S–S bond. These π interactions are quite favorable because of the polarity of the S–F bonds; when the F atoms are substituted for H atoms, the S–S bond lengthens to 2.017 Å for HSSF and to 2.087 Å for HSSH. The analogous MOs for HSSH are shown in Figure 3b, where there is no apparent π bonding character. As a result, the energetic dependence on the dihedral angle is the most pronounced for FSSF, followed by HSSF; this is clear in the potential energy scans as a function of dihedral angle for HSSH, HSSF, and FSSF (Figure 4a).

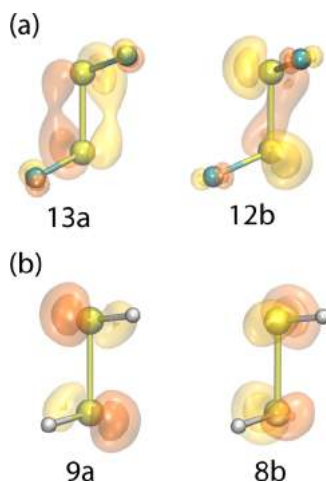


**Figure 3.** Molecular orbitals for the S 3p-like pairs of electrons in (a) FSSF and (b) HSSH.

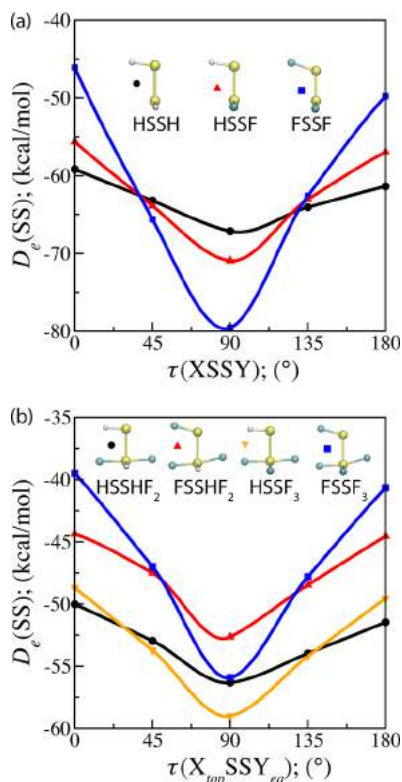


**Figure 4.** (a)  $D_e(SS)$  for XSSY (X, Y = H or F) as a function of dihedral angle ( $\tau$ ) and (b) the corresponding dihedral of XSSYF<sub>2</sub>, where X is bonded to the top sulfur atom and Y is the equatorially oriented atom.

The barriers are listed in Table 4 for rotation involving the parallel and antiparallel alignment of the S–X (X = H or F) bonds, where the difference between the two alignments is relatively small.

Given the potential for unfavorable steric and electrostatic interactions between  $F_{cis}$  and  $F_{top}$ , it may be surprising that these atoms are aligned with one another [ $\tau(F_{top}-S-S-F_{cis}) = 4.4^\circ$ ] in the optimal FSSF<sub>3</sub> (a) geometry. However, from the recoupled pair bonding perspective, this is to be expected based on the properties of the parent FSSF molecule, in which  $\tau(F-S-S-F) = 87.9^\circ$ . It is favorable for  $F_{top}$  and  $F_{eq}$  to be oriented at

**Table 4.** Barriers for Parallel and Antiparallel Rotation for XSSY and XSSYF<sub>2</sub> (X, Y = H or F) Relative to the Orientation of  $X_{top}$  and  $Y_{eq}$  in the Latter

	parallel (kcal/mol)	antiparallel (kcal/mol)
HSSH	8.0	5.8
HSSF	15.3	14.0
FSSF	33.5	29.8
HSSHF <sub>2</sub>	6.3	4.9
FSSHF <sub>2</sub>	8.5	8.3
HSSF <sub>3</sub>	10.3	9.5
FSSF <sub>3</sub>	16.6	15.4

about  $90^\circ$  to optimize  $\pi$ -like interactions [ $\tau(F_{top}-S_{top}-S_{hyp}-F_{eq}) = 94.6^\circ$ ]. Because one of the delocalized S 3p<sup>2</sup>-like pairs from FSSF must form a recoupled pair bond dyad with two F atoms to yield FSSF<sub>3</sub> (a), the barrier to rotation is diminished (see Table 4 and Figure 4b) and the S–S bond is lengthened in FSSF<sub>3</sub> (a) relative to FSSF. Even though one of the  $\pi$ -like interactions in FSSF is removed, the  $F_{trans}$  atom can interact in a similar way with the electron-deficient region of  $S_{top}$ , which is manifest in  $F_{trans}$  tilting upward toward  $S_{top}$  in FSSF<sub>3</sub> (a) and FSSHF<sub>2</sub>; see the structures in Figure 4b.

Because the effects that favor a  $F_{top}$  and  $F_{eq}$  orientation of approximately  $90^\circ$  (interaction of  $F_{trans}$  and  $S_{top}$  and polarization of the remaining 3p<sup>2</sup>-like pair toward  $S_{hyp}$ ) work in tandem, FSSF<sub>3</sub> (a) has the largest barrier to rotation. By comparing the barrier to rotation in HSSF<sub>3</sub> and FSSHF<sub>2</sub>, we can discern that the 3p<sup>2</sup>-like  $\pi$  interaction is somewhat more stabilizing than the  $S_{top}-F_{trans}$  interaction because the barrier to rotation in HSSF<sub>3</sub> is slightly larger than that in FSSHF<sub>2</sub>. Despite FSSF<sub>3</sub> (a) having the largest barrier to rotation, HSSF<sub>3</sub> has the strongest S–S bond; this can be rationalized by the favorable electrostatic interactions between  $H_{top}$  and  $F_{cis}$  as well as reduced steric interactions between  $H_{top}$  and the SF<sub>3</sub> group. While the HSSHF<sub>2</sub> curve is relatively flat, it also has a stronger S–S bond than FSSF<sub>3</sub> (a).

The average  $D_e$  of the axial bonds of FSSF<sub>3</sub> (a),  $D_e(SF_{ax}) = 1/2[D_e(S_{hyp}-F_{cis}) + D_e(S_{hyp}-F_{trans})]$ , is reduced relative to the bonds in SF<sub>2</sub>(<sup>3</sup>B<sub>1</sub>) (62.3 versus 72.2 kcal/mol). A portion of this destabilization is certainly due to the weaker S–S bond in FSSF<sub>3</sub> (a) that results from recoupling the electrons in the 3p<sup>2</sup>-like lone pair of FSSF. We can approximately adjust the calculation of  $D_e(SF_{ax})$  to reflect only the change in stability of the S–F dyad bonds in FSSF<sub>3</sub> (a) by adding in the difference in S–S bond energy of HSSH, which is much closer to a single S–S bond, from that of FSSF ( $\Delta E = 12.5$  kcal/mol) to the bond dissociation energy calculation. This yields an adjusted  $D_e(SF_{ax})$  of 69.5 kcal/mol, which is reasonably close to the bonds in SF<sub>2</sub>(<sup>3</sup>B<sub>1</sub>). This comparison indicates that covalent addition of the  $F_{eq}$  atom and the  $S_{top}-F_{top}$  fragment to SF<sub>2</sub>(<sup>3</sup>B<sub>1</sub>) only slightly destabilizes the recoupled pair bond dyad. These bonds do not appreciably increase the repulsion between the electron pairs surrounding  $S_{hyp}$ , which is a key to obtaining stable p<sup>2</sup>-mediated recoupled pair bonds and dyads.<sup>8</sup> In the next section, we will see that this consideration explains many of the features of the higher-lying rotamer, FSSF<sub>3</sub> (b).

**B. FSSF<sub>3</sub> (b).** There is a higher-lying ( $\Delta E = 18.0$  kcal/mol) isomer of FSSF<sub>3</sub>, denoted here as FSSF<sub>3</sub> (b); see Figure 2. In this isomer, an SF group and a F atom are bonded to  $S_{hyp}$  in the axial positions, and both equatorial (i.e., covalently bound) positions are occupied by F atoms. This isomer possesses C<sub>1</sub>

symmetry (deviating only slightly from  $C_s$  symmetry), and the barrier to rotation (6.3 kcal/mol) is markedly reduced relative to FSSF<sub>3</sub> (a) in accordance with the longer S–S bond noted above. As in FSSF<sub>3</sub> (a), the axial bonds comprise a recoupled pair bond dyad. The GVB orbitals associated with the axial bonds for FSSF<sub>3</sub> (a) and FSSF<sub>3</sub> (b) are shown in Figure 5. The

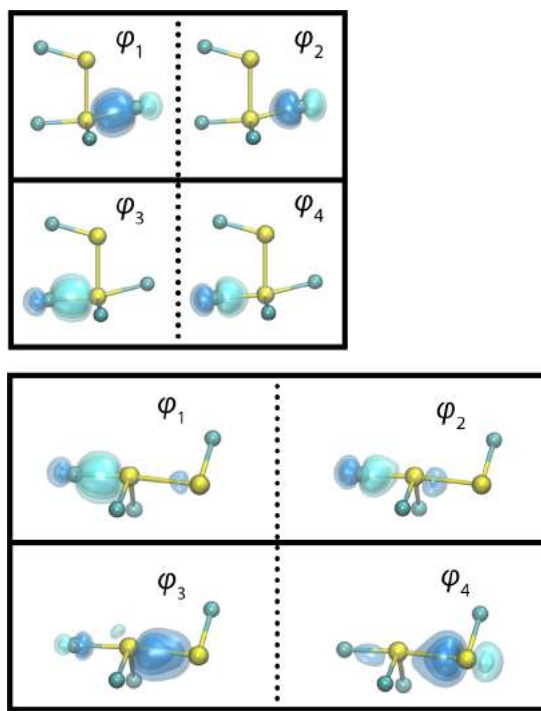


**Figure 5.** GVB orbitals for the axial bonds of FSSF<sub>3</sub> (a), upper panels, and FSSF<sub>3</sub> (b), lower panels; throughout the figures, the dashed lines indicate that a pair is singlet coupled in the wave function.

orbitals (and their overlaps, see Table S4 in the Supporting Information) in both isomers are quite similar because of the energetic incentive to reduce Pauli repulsion among the nonpaired electrons in the dyad. However, achieving this electronic structure is less energetically favorable in FSSF<sub>3</sub> (b) than in FSSF<sub>3</sub> (a) because it requires that the electron-poor  $S_{hyp}$  atom donate electron density to the  $S_{ax}-F_{ax}$  group to minimize unfavorable overlaps ( $S_{13}$  in particular; see  $\phi_3$  in Figure 5, lower panels). As a result, the  $S_{ax}-F_{ax}$  group is negatively charged (−0.24) and the  $SF_3$  group is equally positively charged, which is clearly not optimal based on the electronegativities of the constituent atoms. In FSSF<sub>3</sub> (a), the opposite is true, as electron density from the  $S_{top}-F_{top}$  group can be donated to  $S_{hyp}$ , giving the  $S_{top}-F_{top}$  group a charge of +0.15. Therefore, in FSSF<sub>3</sub> (a), there is a good match between the ability of the electrons in the recoupled orbitals to avoid one another and the optimal charge distribution for the molecule relative to the constituent atoms. Additionally, the GVB orbitals associated with FSSF<sub>3</sub> (b) appear to contain a small amount of antibonding character. This suggests that, despite the similarities in the GVB overlaps, the spatial separation of the bonds in the dyad is not as complete in FSSF<sub>3</sub> (b) relative to FSSF<sub>3</sub> (a), a reflection of the reduced electronegativity of the SF group relative to a bare F atom.

In Table 3, we report a bond dissociation energy of 53.3 kcal/mol for this S–S bond, relative to  $SF(^2\Pi) + SF_3(const)$ , where the  $F_{eq}-S_{hyp}-F'_{eq}$  angle of  $SF_3(const)$  is fixed at its value

in  $SF_2(^1A_1)$ . This results in an  $SF_3$  structure with two polar covalent bonds and a single recoupled pair bond between the S  $3p^2$  pair of  $SF_2(^1A_1)$  and the incoming F  $2p^1$  orbital.<sup>8</sup> In this way, the bonding motif of FSSF<sub>3</sub> (b) is already present within the fragments, so the dissociation energy reflects only the strength of the bond and not the significant electronic rearrangement of the parent fragments,  $SF_3$  in particular.<sup>7</sup> With halogen ligands, we have generally found that the bonds that complete a recoupled pair bond dyad are quite strong, often stronger than their covalent analogues.<sup>37</sup> For example, the dissociation energy for an axial bond of  $SF_4(^1A')$  relative to  $F(^2P) + SF_3(const)$  is 114.7 kcal/mol, compared to 84.5 kcal/mol for  $SF(^2\Pi)$  at the same level of theory! Given this consideration, this S–S bond is actually weaker than might be anticipated, a result of the reduced electronegativity of the  $S_{ax}-F_{ax}$  group in the dyad position.

In prior work, the relative instability of FSSF<sub>3</sub> (b) was attributed to the long S–S bond and repulsion between the nonbonded  $3s$ -like pair of  $S_{hyp}$  and the  $S_{ax}-F_{ax}$  group.<sup>2</sup> However, recoupled pair bonds and dyads tend to be longer than their covalent analogues.<sup>37</sup> Therefore, the elongated S–S bond is an expected consequence of recoupled pair bonding and not by itself necessarily destabilizing. Moreover, it seems unlikely that lone pair repulsion is a significant effect because the energies of the parallel and antiparallel transition states associated with FSSF<sub>3</sub> (a) rotation are so close ( $\Delta E = 1.2$  kcal/mol); the S–S bonds are in fact a bit shorter in these geometries (2.198 Å for the parallel configuration and 2.173 Å for the antiparallel alignment) than in FSSF<sub>3</sub> (b). To further investigate this, we substituted the F atom of the  $S_{ax}-F_{ax}$  group with a larger Cl atom to see if it is more destabilizing; the SS bond in ClSSF<sub>3</sub> (b) is 52.9 kcal/mol, compared to 53.3 kcal/mol in FSSF<sub>3</sub> (b). We also investigated the hydrogenated analog, HSSF<sub>3</sub> (b), which has an S–S bond energy of 58.0 kcal/mol and is 16.2 kcal/mol above HSSF<sub>3</sub> (a)—very similar to the fluorinated analog. These calculations support our conclusion that the suboptimal charge distribution in FSSF<sub>3</sub> (b), and not steric effects, is largely the reason for the instability of FSSF<sub>3</sub> (b) relative to FSSF<sub>3</sub> (a).

**C. SSF<sub>4</sub>.** SSF<sub>4</sub> is intermediate in energy between FSSF<sub>3</sub> (a) and FSSF<sub>3</sub> (b), lying 6.9 kcal/mol above FSSF<sub>3</sub> (a) and 11.1 kcal/mol below FSSF<sub>3</sub> (b). While this species has not been observed experimentally, the oxygen-substituted analog, F<sub>4</sub>SO, is a well-known molecule.<sup>3,38</sup> At a lower level of theory, SSF<sub>4</sub> dissociates into S + SF<sub>4</sub>, but more recent calculations have shown that SSF<sub>4</sub> is in fact stable with respect to this asymptote.<sup>2</sup> The optimized geometry of SSF<sub>4</sub> has a short S–S bond length of 1.904 Å. The participation of d-orbitals has been invoked to account for the shortness of this bond via  $\pi$ -d back bonding;<sup>2</sup> however, d-orbitals have been shown repeatedly to be too high in energy to act as valence orbitals in hypervalent sulfur-containing species.<sup>39–41</sup> While the S–S bond length is consistent with species like FSSF and S<sub>2</sub> [1.919, 1.913(<sup>3</sup> $\Sigma_g^-$ ), 1.915(<sup>1</sup> $\Delta_g$ ) Å, respectively], SSF<sub>4</sub> has a S–S bond energy notably weaker than that of these compounds. The S–S bond energies for FSSF, S<sub>2</sub>(<sup>3</sup> $\Sigma_g^-$ ), and S<sub>2</sub>(<sup>1</sup> $\Delta_g$ ) are 79.6, 102.4, and 86.0 kcal/mol, respectively. Meanwhile, SSF<sub>4</sub> is only 63.2 kcal/mol below the lowest asymptote that can form a singlet state:  $S(^1D) + SF_4(^1A')$  (Table 3). These two fragments could interact to form a dative bond with the polarized  $3s^2$ -like lone pair of SF<sub>4</sub> and the empty  $3p$  orbital of  $S(^1D)$ , resulting from mixing with  $S(^1S)$ . Consistent with this bonding scheme, the geometry of the SF<sub>4</sub> group in SSF<sub>4</sub> is structurally similar to that

of  $\text{SF}_4(^1\text{A}')$ . Additionally, the charge distribution is consistent with electron density being donated to  $\text{S}_{\text{ter}}$ , with a charge of  $-0.20$  on this atom.

However, the relative weakness of the S–S bond (given its shortness) suggests that a dative (single) S–S bond may not be a complete description. Moreover, while dative bonds are stabilized by a polarizable lone pair of electrons on the donor molecule and an electronegative ligand for the acceptor, in  $\text{SF}_4(^1\text{A}')$ , the sulfur atom has a Mulliken charge of  $+1.84$ , which should dramatically decrease the polarizability of the distorted 3s-like orbital. Furthermore, the sulfur atom is not especially electronegative relative to another sulfur atom, particularly one that is positively charged. The GVB orbitals in Figure 6 provide

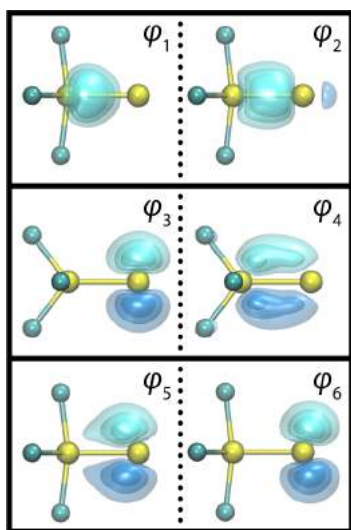


**Figure 6.** GVB orbitals associated with the S–S  $\sigma$  bond (top panels) and the  $\pi$  orbitals aligned perpendicular to (middle panels) and with (bottom panels) the axial SF bonds.

additional insight into the nature of the S–S bond in  $\text{SSF}_4$ . The S–S bond pair has one orbital that correlates well with an S 3s lobe orbital ( $\varphi_1$ ), and the other orbital is delocalized over the bond pair ( $\varphi_2$ ); this is consistent with the formation of a dative  $\sigma$  bond. Aligned with the axial S–F bonds, we find two  $\text{S}_{\text{ter}}$ -centered 3p lobes ( $\varphi_5, \varphi_6$ ) that are essentially an S  $3p^2$  pair with slight polarization toward  $\text{S}_{\text{hyp}}$ . This is also consistent with what we would expect for a dative S–S bond. However, in the orthogonal direction, the p orbitals are qualitatively different. The orbitals ( $\varphi_3, \varphi_4$ ) are substantially more polarized toward  $\text{S}_{\text{hyp}}$  to the extent that one of the GVB orbitals ( $\varphi_4$ ) appears to originate from  $\text{S}_{\text{hyp}}$  and not  $\text{S}_{\text{ter}}$ . An  $\text{S}_{\text{hyp}}$ -centered orbital in the  $\pi$  space implies formation of a  $\pi$  bond. Thus, the GVB calculations indicate that the S–S bond has significant double-bond character, as opposed to exclusively a single dative bond.

An asymptote that is consistent with this bonding pattern is  $\text{S}(^3\text{P}) + \text{SF}_4(^3\text{A}'')$ ; the structure of the latter species is shown in Figure 2.  $\text{SF}_4(^3\text{A}'')$  is weakly bound, lying only 4.2 kcal/mol below the  $\text{F}(^2\text{P}) + \text{SF}_3(^2\text{A}')$  asymptote. The singly occupied, triplet-coupled orbitals are shown in Figure 7, as is the polarized 3s<sup>2</sup>-like nonbonding pair of  $\text{SF}_4(^1\text{A}')$  for comparison. The unpaired orbitals from  $\text{SF}_4(^3\text{A}'')$  bear a strong resemblance to the two sulfur-centered orbitals of  $\text{SSF}_4$ ,  $\varphi_1$  and  $\varphi_4$  in Figure 6. The main difference is that the orbitals of  $\text{SSF}_4$  have lost antibonding character by polarizing toward  $\text{S}_{\text{ter}}$ . From this

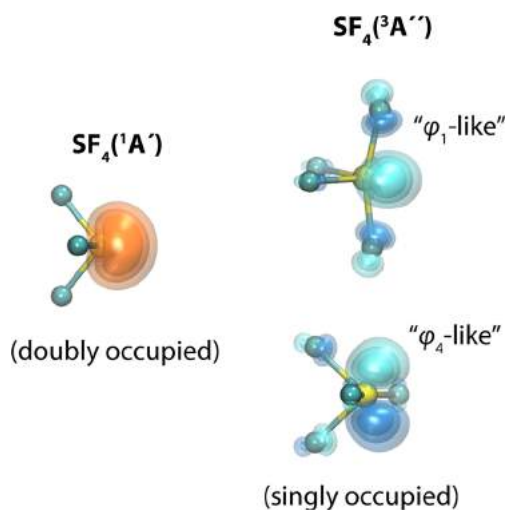


**Figure 7.** Nonbonding sulfur-centered molecular orbitals of the (a) ground  $^1\text{A}'$  state and (b) excited  $^3\text{A}''$  state of  $\text{SF}_4$  in relation to the orbitals for  $\text{SSF}_4$  shown in Figure 6.

asymptote,  $\text{S}(^3\text{P})$  can form two bonds, a  $\sigma$  and a  $\pi$  bond, with  $\text{SF}_4(^3\text{A}'')$ . However, this asymptote is considerably higher in energy, lying 66.3 kcal/mol above the  $\text{S}(^1\text{D}) + \text{SF}_4(^1\text{A}')$  asymptote. Along with a more detailed description of the bonding in  $\text{SF}_4(^3\text{A}'')$ , in the Supporting Information (Figure S1 and Section S.IV), we assess the energetic considerations associated with the bonding from this asymptote. Our analysis indicates that this asymptote could indeed influence the S–S bond in  $\text{SSF}_4$ , resulting in the GVB orbitals shown in Figure 6 and contributing to the shorter S–S bond length and orbital delocalization present in  $\text{SSF}_4$ , in conjunction with contributions from the dative bonded asymptote. A favorable bonding interaction from a higher-lying asymptote that is capable of forming an additional bond could also account for the closeness in energy of  $\text{SSF}_4$  and  $\text{FSSF}_3$  (a) [ $\Delta E = 6.9$  kcal/mol], which at first glance may be surprising given that the lowest-lying asymptote of  $\text{SSF}_4$  requires an appeal to a higher-lying ( $\Delta E$  of at least 29.0 kcal/mol) asymptote while  $\text{FSSF}_3$  (a) does not. This is similar in spirit to our previous work on  $\text{Cl}_2\text{SO}$ , in which we showed that the higher-lying triplet states of  $\text{Cl}_2\text{S}$  bonding to the  $\text{O}(^3\text{P})$  atom were largely responsible for the strength and length of the S–O bond.<sup>42</sup>

Additional evidence for the importance of the triplet asymptote on  $\text{SSF}_4$  comes by way of comparison to the fully hydrogen-substituted analog,  $\text{SSH}_4$ , which possesses a similar structure. However, there is no minimum for  $\text{SH}_4(^3\text{A}'')$  with an analogous structure to that of  $\text{SF}_4(^3\text{A}'')$ . The dative bonding from  $\text{S}(^1\text{D}) + \text{SH}_4(^1\text{A}')$ , on the other hand, is expected to be more favorable in this case because of the increased polarizability of the 3s-like orbital on the  $\text{SH}_4$  fragment. The S–S bond in the hydrogenated species is notably longer [ $R(\text{SS}) = 2.001$  Å] but slightly stronger [ $D_e(\text{SS}) = 66.3$  kcal/mol] than that in  $\text{SSF}_4$ . Generally, bond lengths and strengths are inversely correlated,<sup>43</sup> but we can rationalize this discrepancy in the context of the above analysis: the increased length is due to the lack of multibond character in  $\text{SSH}_4$ , but the slightly larger bond energy is due to the increased favorability of dative bonding.

**D.  $\text{F}_2\text{SSF}_2$ .** Before the structure of  $\text{FSSF}_3$  (a) was elucidated, alternative structures were proposed for the product of  $\text{SF}_2$  dimerization that had two F atoms bonded to each sulfur atom.

However, higher-level calculations have shown these geometries to be saddle points rather than minima on the potential energy surface.<sup>2</sup> In Figure 2, we show two such stationary points ( $^1A_g$  and  $^1A'$ ). Interestingly, they have S–S bond lengths typical of single bonds and are stable with respect to S–S stretching. The SF<sub>2</sub> fragments in the F<sub>2</sub>SSF<sub>2</sub> molecules are extremely similar in structure to the  $^3B_1$  state of SF<sub>2</sub> (see Table 1b and Figure 2). As shown in Figure 1, the SF<sub>2</sub>( $^3B_1$ ) state has two singly occupied orbitals ( $a_1$  and  $b_1$ ). Therefore, there is potential for forming double bonds between the two S atoms by two mechanisms.

(1) We can align the singly occupied  $b_1$  symmetric orbitals of the two SF<sub>2</sub>( $^3B_1$ ) states to form a  $\sigma$  bond, yielding the  $C_s$  symmetric structure in Figure 2 [labeled F<sub>2</sub>SSF<sub>2</sub>( $^1A'$ )], which is a first-order saddle point. This transition state connects two stereoisomers of FSSF<sub>3</sub>(a) with structures along the intrinsic reaction coordinate possessing an F<sub>2</sub>SSF<sub>2</sub> bonding motif seen in prior work:<sup>5</sup> the S 3p<sup>2</sup>-like orbital of a ground-state SF<sub>2</sub>( $^1A_1$ ) fragment forms a dative bond with a singlet analogue of SF<sub>2</sub>( $^3B_1$ ). Because the S 3p-like singly occupied orbitals that are not involved in the recoupled pair bond dyad are singlet (instead of triplet) coupled in the latter fragment, one of the S 3p-like orbitals can be unoccupied and therefore accept an electron pair from the ground state SF<sub>2</sub>( $^1A_1$ ) fragment.

(2) Alternatively, we can align the  $a_1$  symmetric orbitals of the two SF<sub>2</sub>( $^3B_1$ ) states to form the  $\sigma$  bond, yielding the  $C_{2h}$  symmetric second-order saddle point shown in Figure 2 [labeled F<sub>2</sub>SSF<sub>2</sub>( $^1A_g$ )]. See Section S.V and Figure S2 in the Supporting Information for more details.

It is now obvious why these structures are significantly higher in energy than the FSSF<sub>3</sub> structures (see Table 2): there is an energetic cost to recoupling the S 3p<sup>2</sup> electrons and forming the dyad (32.5 kcal/mol in SF<sub>2</sub>; see Figure 1), and in the F<sub>2</sub>SSF<sub>2</sub> structures, two S 3p pairs must be recoupled, whereas only one S 3p<sup>2</sup> pair must be recoupled to form FSSF<sub>3</sub>.

It merits comment that by forming a  $\sigma$  bond between two SF<sub>2</sub>( $^3B_1$ ) fragments, the orbitals that do not participate in the  $\sigma$  bond are aligned such that they can form a  $\pi$  bond. However, the S–S bonds in F<sub>2</sub>SSF<sub>2</sub> structures are notably weaker and longer than would be expected for an S–S double bond: they are stable with respect to two SF<sub>2</sub>( $^3B_1$ ) molecules by only 35.5 and 37.3 kcal/mol (Table 3) with S–S bond lengths of 2.100 and 2.102 Å (Table 1b). When selected GVB orbitals are analyzed for these structures, we do in fact find  $\sigma$  and  $\pi$  S–S bonds. For F<sub>2</sub>SSF<sub>2</sub>( $^1A_g$ ), this bonding pattern described the majority (96.4%) of the wave function, with favorable overlaps of 0.80 and 0.51 for the  $\sigma$  and  $\pi$  bonds, respectively (Figure 8). (The analogous orbitals for F<sub>2</sub>SSF<sub>2</sub>( $^1A'$ ) are very similar; see Figure S3 in the Supporting Information.) There are several reasons for the weakness of the S–S bonds in the two singlet F<sub>2</sub>SSF<sub>2</sub> structures. (1) As we saw in the barriers to rotation for FSSF<sub>3</sub>, steric or electrostatic repulsion is not a large effect at longer S–S bond lengths. But this repulsion will increase in magnitude as the S–S bond shrinks, especially given that there are now two pairs of F atoms aligned with one another in the F<sub>2</sub>SSF<sub>2</sub> species. (2) Because both S atoms are bonded to two F atoms and form recoupled pair bond dyads, they both have rather large positive charges (e.g., +1.14 in the  $C_{2h}$  symmetric structure) associated with them. In both FSSF<sub>3</sub> isomers, the SF group containing the nonhypervalent sulfur was able to respond to stabilize bonding around S<sub>hyp</sub>, but here each sulfur atom participates in a recoupled pair bond dyad, so this cannot occur.

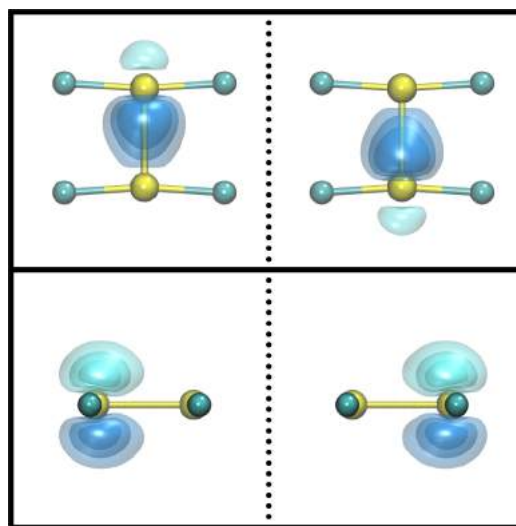


Figure 8. GVB orbitals for the  $\sigma$  and  $\pi$  bonds in F<sub>2</sub>SSF<sub>2</sub>( $^1A_g$ ).

These effects favor longer S–S bond lengths to minimize steric and electrostatic repulsion. At larger S–S bond lengths, the bonding orbitals cannot favorably overlap as much. Because of their orientation, the strengths of  $\pi$  bonds are especially distance-dependent. So, if steric and/or electrostatic effects keep the SF<sub>2</sub> fragments from approaching closely, then both bonds, but the  $\pi$  bond in particular, will be markedly weaker. For instance, if the GVB wave function is computed at an optimized F<sub>2</sub>SSF<sub>2</sub> geometry of  $C_{2h}$  symmetry where  $R(SS)$  is constrained to be 1.915 Å [that of S<sub>2</sub>( $^1\Delta_g$ )], the  $\sigma$  overlap increases to 0.85, for a gain of 0.05. The  $\pi$  overlap is even more affected, increasing by 0.10 to a value of 0.61. However, these energetic gains in the bonding orbitals are more than negated by the increased repulsion as mentioned above. (The distance between fluorine atoms on the opposite sulfur atoms decreases by 0.05 Å in the constrained geometry relative to the fully optimized structure.) One final effect that contributes to the small  $D_e(SS)$  values in Table 3 is the loss of triplet coupling on both SF<sub>2</sub>( $^3B_1$ ) fragments; the  $^3B_1 \rightarrow ^1A_1$  energy gap is 18.7 kcal/mol at the  $^3B_1$  minimum. This reduces the calculated bond energy relative to this asymptote.

The above F<sub>2</sub>SSF<sub>2</sub> stationary points have an interesting analogue on the triplet surface. A  $\sigma$  bond between the  $b_1$  symmetric orbitals of SF<sub>2</sub>( $^3B_1$ ) can be formed in the F<sub>2</sub>SSF<sub>2</sub>( $^3B$ ) state in the same fashion as in the F<sub>2</sub>SSF<sub>2</sub>( $^1A'$ ) state. However, the electrons in the  $a_1$  symmetric orbitals of SF<sub>2</sub>( $^3B_1$ ) are now coupled into high spin, and therefore the SF<sub>2</sub> groups are perpendicular to one another so that the triplet-coupled orbitals have zero overlap. In this configuration the lone pair orbitals on the F atoms avoid each other because there is no  $\pi$  bond to favor their alignment. This structure, F<sub>2</sub>SSF<sub>2</sub>( $^3B$ ), is a true minimum, and its normal modes are shown in Figure 9. The S–S bond is longer and weaker than on the singlet surface (see Tables 1b and 3) because of the loss of the  $\pi$  interaction, but this effect is small because of (1) the weakness of the  $\pi$  interactions in the singlet state, (2) the reduction in unfavorable interactions between the lone pairs on the F atoms, and (3) the exchange energy resulting from the triplet coupling (the  $^3B \rightarrow ^1A$  gap is 8.3 kcal/mol at this geometry). This structure is metastable with respect to the lowest asymptote, being 2.9 kcal/mol above the SF<sub>2</sub>( $^1A_1$ ) + SF<sub>2</sub>( $^3B_1$ ) asymptote, but it is bound by 29.1 kcal/mol relative to

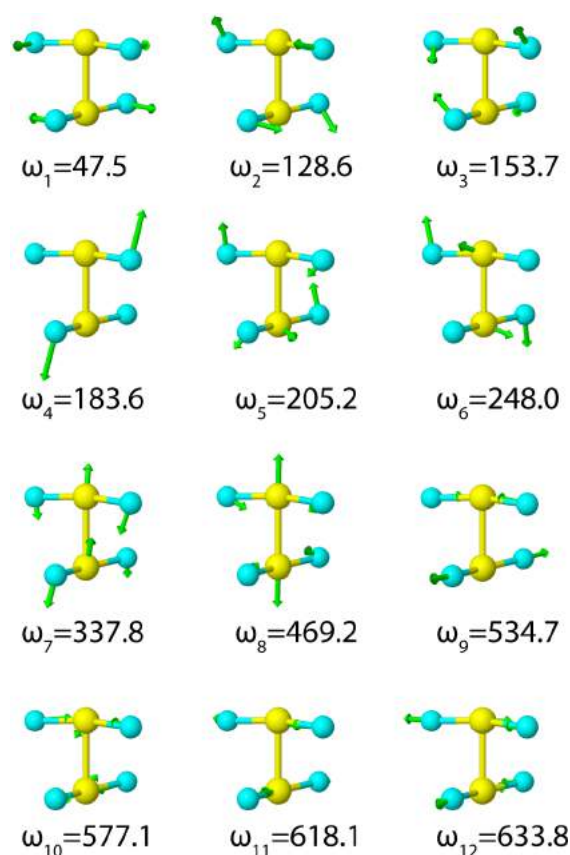


Figure 9. Normal modes for  $F_2SSF_2(^3B)$ .

two  $^3B_1$   $SF_2$  molecules. No low-energy paths to form  $F_2SSF_2(^3B)$  were located, so this minimum is mainly of theoretical interest, but it demonstrates the utility of the recoupled pair bonding framework in predicting previously unknown, and perhaps nonintuitive, structures.

#### IV. CONCLUSIONS

We investigated the bonding of various  $S_2F_4$  structures: two FSSF<sub>3</sub> isomers, one SSF<sub>4</sub> structure, and three stationary points with  $F_2SSF_2$  connectivity (two saddle points and one minimum). Our results are in good agreement with prior studies, and we expanded upon this literature by thoroughly analyzing the bonding of the  $S_2F_4$  structures with GVB theory and the associated recoupled pair bonding model, as well as by reporting a novel minimum associated with the triplet state of  $F_2SSF_2$ . The nature of the bonding in the FSSF<sub>3</sub> structures and the SSF<sub>4</sub> structure were firmly grounded in calculations of the GVB wave function associated with each of the geometries. Moreover, the origin of the stability with respect to S–S distance for the  $F_2SSF_2$  structures is clear within the context of our prior work on the  $SF_2$  molecule, particularly the electronic structure of the  $^3B_1$  state of  $SF_2$ .

We have shown that fluorine and sulfur can bond to form many configurations because these two atoms are well suited to form recoupled pair bonds as well as polar covalent bonds. The different bonding motifs available can be seen by considering the character of the S–S bonds in these species, where we have observed (1) a typical covalent bond [FSSF<sub>3</sub> (a),  $F_2SSF_2(^3B)$ ], (2) a weak double bond [ $F_2SSF_2(^1A')$ ,  $F_2SSF_2(^1A_g)$ ], (3) a member of a recoupled pair bond dyad [FSSF<sub>3</sub> (b)], and (4) an S → S(<sup>1</sup>D) dative bond that is likely strengthened by a strong

double bond originating from a higher-lying asymptote [SSF<sub>4</sub>]. Although the F–S–F recoupled pair bond dyad is stronger than expected, it is still weaker than a pair of polar covalent bonds, by 32.5 kcal/mol in  $SF_2$ . Therefore, the relative energetics of the  $S_2F_4$  species are influenced by the number of recoupled pair bond dyads required to form them and the resulting charge distribution relative to the constituent atoms, with FSSF<sub>3</sub> (a) being optimal in this regard.

In addition to deepening our understanding of the rich diversity of sulfur fluoride chemistry, this work underscores the ability of GVB theory in conjunction with the recoupled pair bonding model to both explain and predict interesting features of sulfur-based molecules. GVB calculations are particularly powerful in their ability to connect features of the constituent fragments to those of the bonded molecule, here lending detailed insight into the character of the bonds of the sulfur difluoride dimer.

#### ■ ASSOCIATED CONTENT

##### Supporting Information

Weights corresponding to the Kotani spin functions for the GVB calculations, comparison of Mulliken and NBO charges, comparison of optimized FSSF<sub>3</sub> (a) geometries using B3LYP/aug-cc-pVTZ and CCSD(T)-F12/aug-cc-pV(D+d)Z, GVB orbital overlaps for FSSF<sub>3</sub> (a) and FSSF<sub>3</sub> (b), energetic considerations related to the contribution of the S(<sup>3</sup>P) + SF<sub>4</sub>(<sup>3</sup>A'') asymptote to formation of SSF<sub>4</sub>, normal modes for  $F_2SSF_2(^1A_g)$ , and GVB orbitals for the S–S bond in  $F_2SSF_2(^1A')$ . This material is available free of charge via the Internet at <http://pubs.acs.org>.

#### ■ AUTHOR INFORMATION

##### Corresponding Author

\*E-mail: thdjr@uw.edu.

##### Present Address

<sup>§</sup>T.H.D.: Pacific Northwest National Laboratory & University of Washington, Northwest Institute for Advanced Computing, Box 352500, Seattle, WA 98195–2500 and University of Washington, Department of Chemistry, Box 351700, Seattle, WA 98195–1700.

##### Notes

The authors declare no competing financial interest.

#### ■ ACKNOWLEDGMENTS

This work was supported by the Distinguished Chair for Research Excellence in Chemistry and the National Center for Supercomputing Applications at the University of Illinois at Urbana–Champaign. One of the authors (B.A.L.) is the grateful recipient of a National Science Foundation Graduate Research Fellowship. A.L.E. was supported through the Summer Research Experience for Undergraduates program, which is supported by U.S. National Science Foundation and the 3M Foundation.

#### ■ REFERENCES

- (1) Griffin, G. D.; Ryan, M. S.; Kurka, K.; Nolan, M. G.; Sauer, I.; James, D. R. Disulfur Decafluoride ( $S_2F_{10}$ ): A Review of the Biological Properties and Our Experimental Studies of This Breakdown Product of  $SF_6$ . In *Gaseous Dielectrics VI*; Christophorou, L. G., Sauer, I., Eds.; Plenum Press: New York, 1991; pp 545–552.
- (2) Steudel, Y.; Steudel, R.; Wong, M. W.; Lentz, D. An Ab Initio MO Study of the Gas-Phase Reactions  $2 SF_2 \rightarrow FS-SF_3 \rightarrow S=SF_4 -$

Molecular Structures, Reaction Enthalpies and Activation Energies. *Eur. J. Inorg. Chem.* **2001**, 2543–2548.

(3) Carlowitz, M. V.; Oberhammer, H.; Willner, H.; Boggs, J. E. Structural Determination of a Recalcitrant Molecule ( $S_2F_4$ ). *J. Mol. Struct.* **1983**, *100*, 161–177.

(4) Gombler, W.; Haas, A.; Willner, H. The Unusual Chemical Equilibria  $F_3S-SF \rightleftharpoons 2 SF_2$  and  $CF_3SF_2-SCF_3 \rightleftharpoons 2CF_3SF$ . *J. Fluorine Chem.* **1980**, *16*, 569–570.

(5) Lindquist, B. A.; Dunning, T. H. Bonding in  $FSSF_3$ : Breakdown in Bond Length-Strength Correlations and Implications for  $SF_2$  Dimerization. *J. Phys. Chem. Lett.* **2013**, *4*, 3139–3143.

(6) Woon, D. E.; Dunning, T. H. A Comparison between Polar Covalent Bonding and Hypervalent Recoupled Pair Bonding in Diatomic Chalcogen Halide Species  $\{O,S,Se\} X \{F,Cl,Br\}$ . *Mol. Phys.* **2009**, *107*, 991–998.

(7) Woon, D. E.; Dunning, T. H., Jr. Theory of Hypervalency: Recoupled Pair Bonding in  $SF_n$  ( $n = 1-6$ ). *J. Phys. Chem. A* **2009**, *113*, 7915–7926.

(8) Lindquist, B. A.; Woon, D. E.; Dunning, T. H., Jr. Effects of Ligand Electronegativity on Recoupled Pair Bonds with Application to Sulfurane Precursors. *J. Phys. Chem. A* **2014**, *118*, 5709–5719.

(9) Werner, H. J. Knowles, P. J.; Knizia, G.; Manby, F. R.; Schutz, M.; Celani, P.; Korona, T.; Lindh, R.; Mitrushenkov, A.; Rauhut, G. et al. *MOLPRO*, version 2010.1, a package of ab initio programs; <http://www.molpro.net>.

(10) Frisch, M. J. Trucks, G. W.; Schlegel, H. B.; Scuseria, G. E.; Robb, M. A.; Cheeseman, J. R.; Montgomery, J. A., Jr.; Vreven, T.; Kudin, K. N.; Burant, J. C. et al. *Gaussian 03*, revision D.01; Gaussian, Inc.: Wallingford, CT, 2004.

(11) Becke, A. D. Density-Functional Thermochemistry. III. The Role of Exact Exchange. *J. Chem. Phys.* **1993**, *98*, 5648–5652.

(12) Lee, C. T.; Yang, W. T.; Parr, R. G. Development of the Colle-Salvetti Correlation-Energy Formula into a Functional of the Electron-Density. *Phys. Rev. B: Condens. Matter Mater. Phys.* **1988**, *37*, 785–789.

(13) Miehlich, B.; Savin, A.; Stoll, H.; Preuss, H. Results Obtained with the Correlation-Energy Density Functionals of Becke and Lee, Yang and Parr. *Chem. Phys. Lett.* **1989**, *157*, 200–206.

(14) Dunning, T. H., Jr. Gaussian-Basis Sets for Use in Correlated Molecular Calculations. I. The Atoms Boron through Neon and Hydrogen. *J. Chem. Phys.* **1989**, *90*, 1007–1023.

(15) Woon, D. E.; Dunning, T. H., Jr. Gaussian-Basis Sets for Use in Correlated Molecular Calculations. III. The Atoms Aluminum through Argon. *J. Chem. Phys.* **1993**, *98*, 1358–1371.

(16) Knizia, G.; Adler, T. B.; Werner, H. J. Simplified CCSD(T)-F12 Methods: Theory and Benchmarks. *J. Chem. Phys.* **2009**, *130*, 054104.

(17) Knizia, G.; Werner, H. J. Explicitly Correlated RMP2 for High-Spin Open-Shell Reference States. *J. Chem. Phys.* **2008**, *128*, 154103.

(18) Knowles, P. J.; Hampel, C.; Werner, H. J. Coupled-Cluster Theory for High-Spin, Open-Shell Reference Wave-Functions. *J. Chem. Phys.* **1993**, *99*, 5219–5227.

(19) Manby, F. R. Density Fitting in Second-Order Linear- $r_{12}$  Møller-Plesset Perturbation Theory. *J. Chem. Phys.* **2003**, *119*, 4607–4613.

(20) Adler, T. B.; Knizia, G.; Werner, H. J. A Simple and Efficient CCSD(T)-F12 Approximation. *J. Chem. Phys.* **2007**, *127*, 221106.

(21) Dunning, T. H., Jr.; Peterson, K. A.; Wilson, A. K. Gaussian Basis Sets for Use in Correlated Molecular Calculations. X. The Atoms Aluminum through Argon Revisited. *J. Chem. Phys.* **2001**, *114*, 9244–9253.

(22) Cooper, D. L.; Thorsteinsson, T.; Gerratt, J. Fully Variational Optimization of Modern VB Wave Functions Using the CASVB Strategy. *Int. J. Quantum Chem.* **1997**, *65*, 439–451.

(23) Thorsteinsson, T.; Cooper, D. L.; Gerratt, J.; Karadakov, P. B.; Raimondi, M. Modern Valence Bond Representations of CASSCF Wavefunctions. *Theor. Chim. Acta* **1996**, *93*, 343–366.

(24) Gerratt, J.; Cooper, D. L.; Karadakov, P. B.; Raimondi, M. Modern Valence Bond Theory. *Chem. Soc. Rev.* **1997**, *26*, 87–100.

(25) Heitler, W.; London, F. Interaction Between Neutral Atoms and Homopolar Binding According to Quantum Mechanics. *Z. Phys.* **1927**, *44*, 457–472.

(26) Pauli, W. On the Connection of the Arrangement of Electron Groups in Atoms with the Complex Structure of Spectra. *Z. Phys.* **1925**, *31*, 765–783.

(27) Goodman, L.; Gu, H. B.; Pophristic, V. Flexing Analysis of Ethane Internal Rotation Energetics. *J. Chem. Phys.* **1999**, *110*, 4268–4275.

(28) Hall, M. B. Valence Shell Electron Pair Repulsions and Pauli Exclusion Principle. *J. Am. Chem. Soc.* **1978**, *100*, 6333–6338.

(29) Jensen, J. H.; Gordon, M. S. An Approximate Formula for the Intermolecular Pauli Repulsion between Closed Shell Molecules. II. Application to the Effective Fragment Potential Method. *J. Chem. Phys.* **1998**, *108*, 4772–4782.

(30) Pipek, J.; Mezey, P. G. A Fast Intrinsic Localization Procedure Applicable for Ab Initio and Semiempirical Linear Combination of Atomic Orbital Wave-Functions. *J. Chem. Phys.* **1989**, *90*, 4916–4926.

(31) Goddard, W. A.; Blint, R. J. Generalized Valence Bond View of Molecules;  $BH_n$  Series. *Chem. Phys. Lett.* **1972**, *14*, 616–622.

(32) Hiberty, P. C.; Shaik, S. A Survey of Recent Developments in Ab Initio Valence Bond Theory. *J. Comput. Chem.* **2007**, *28*, 137–151.

(33) Reed, A. E.; Curtiss, L. A.; Weinhold, F. Intermolecular Interactions from a Natural Bond Orbital, Donor–Acceptor Viewpoint. *Chem. Rev. (Washington, DC, U.S.)* **1988**, *88*, 899–926.

(34) Cordero, B.; Gomez, V.; Platero-Prats, A. E.; Reves, M.; Echeverria, J.; Cremades, E.; Barragan, F.; Alvarez, S. Covalent Radii Revisited. *Dalton Trans.* **2008**, 2832–2838.

(35) Haas, A.; Willner, H. Lower Chalcogen Fluorides. IV. Preparation and Characterization of Pure  $S_2F_4$ . *Z. Anorg. Allg. Chem.* **1980**, *462*, 57–60.

(36) Gombler, W.; Schaebbs, J.; Willner, H.  $^{19}F$  NMR Chemical Shift of  $SF_2$  in the Gas Phase. *Inorg. Chem.* **1990**, *29*, 2697–2698.

(37) Dunning, T. H., Jr.; Woon, D. E.; Leiding, J.; Chen, L. The First Row Anomaly and Recoupled Pair Bonding in the Halides of the Late p-Block Elements. *Acc. Chem. Res.* **2013**, *46*, 359–368.

(38) Cunningham, T. P.; Cooper, D. L.; Gerratt, J.; Karadakov, P. B.; Raimondi, M. Chemical Bonding in Oxofluorides of Hypercoordinate Sulfur. *J. Chem. Soc., Faraday Trans.* **1997**, *93*, 2247–2254.

(39) Cooper, D. L.; Cunningham, T. P.; Gerratt, J.; Karadakov, P. B.; Raimondi, M. Chemical Bonding to Hypercoordinate 2nd-Row Atoms: d Orbital Participation Versus Democracy. *J. Am. Chem. Soc.* **1994**, *116*, 4414–4426.

(40) Magnusson, E. Hypercoordinate Molecules of 2nd-Row Elements: d Functions or d Orbitals? *J. Am. Chem. Soc.* **1990**, *112*, 7940–7951.

(41) Magnusson, E. The Role of d Functions in Correlated Wave Functions: Main Group Molecules. *J. Am. Chem. Soc.* **1993**, *115*, 1051–1061.

(42) Lindquist, B. A.; Dunning, T. H., Jr. The Nature of the SO Bond of Chlorinated Sulfur-Oxygen Compounds. *Theor. Chem. Acc.* **2014**, *133*, 1443.

(43) Gordy, W. A Relation between Bond Force Constants, Bond Orders, Bond Lengths, and the Electronegativities of the Bonded Atoms. *J. Chem. Phys.* **1946**, *14*, 305–320.